Chapter 12
Standardised Manufacture of Iron Age Weaponry from Southern Scandinavia: Constructing and Provenancing the Havor Lance

Thomas Birch

Introduction and Archaeological Background

A substantial quantity and variety of weapons from the Late Roman/Early Germanic Iron Age have been found in "war booty sacrifices" known from across southern Scandinavia. The weapons themselves are thought to represent the spoils of war taken from defeated armies and votively deposited as an expression of victory (Jørgensen et al. 2003). The weapon deposits often contain hundreds, if not thousands, of items including weapons and other *militaria*. One of the best recorded weapon deposits, Illerup Ådal, has yielded over 6000 iron objects (out of roughly 15,000 military items) totalling some 500 kg of worked iron, including 748 lances, 661 spears, 150 swords, and 400 shields (Ilkjær 1990a, b, 2000, 2003, 2008). One of the weapon types found in four (out of six) of the main war booty sacrifices investigated in this chapter (i.e. Ejsbøl, Illerup, Nydam, Skedemosse) is the Havor lance, which dates narrowly to around 375–400 CE. A photograph and schematic illustration of the Havor lance can be seen in Fig. 12.1.

The Havor lance has traditionally been considered a standardised product (Ilkjær 1990a). Whilst this may appear so, this study aims to empirically investigate the degree of standardisation of the material(s) and manufacturing technology used to construct it. This chapter follows up from a previous paper that specifically examined the outward appearance of the Havor lance, focusing on traditional metric analysis as well as adopting an innovative approach using geometric morphometric (GMM) analysis (Birch and Martinón-Torres in press). The paper aimed to investigate the degree of similarity or difference between Havor lances in terms of metric dimensions and overall shape. Overall, 123 lances were examined from three of the main weapon deposits (Bemmann and Bemmann 1998a, b; Ilkjær 1990a, b; Ørsnes

T. Birch (✉)
Centre for Urban Network Evolutions (UrbNet), Aarhus University, Moesgaard Allé 20, 4230, 2nd floor, Højbjerg DK-8270, Denmark

A. Dolfini et al. (eds.), *Prehistoric Warfare and Violence*,
Quantitative Methods in the Humanities and Social Sciences,
https://doi.org/10.1007/978-3-319-78828-9_12

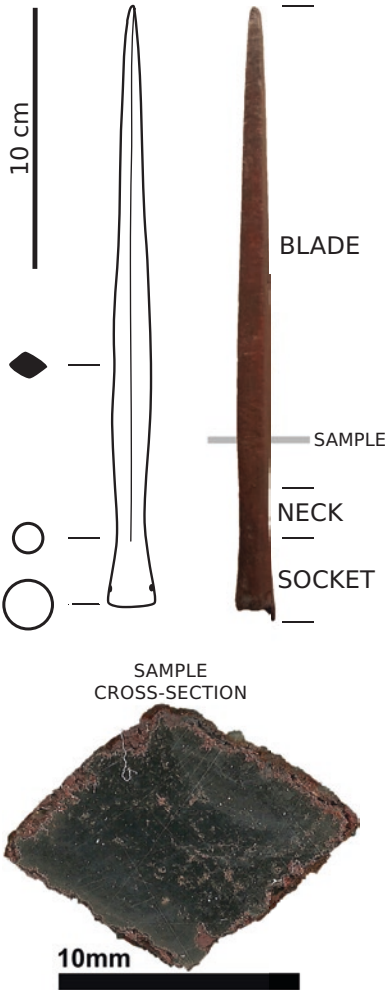

Fig. 12.1 Photograph (right) and schematic illustration (left) of the Havor lance (example E1338), highlighting the area sampled and the cross-section (bottom) obtained

1988), and the results confirmed the Havor lance type to be a highly standardised and symmetrical weapon product, with no significant statistical difference between sites.

This chapter takes the discussion further by examining the relationship between the outward appearance of the lance and its internal make-up, in terms of both material and manufacturing technology. The aim is to assess the degree of internal standardisation of the specimens examined. The results are important for shedding further light on the organisation of weapon manufacturing practices, as well as their material sources, during the Iron Age of southern Scandinavia.

Methods and Materials

Thirteen lances were available for study, twelve newly sampled lanceheads from Ejsbøl (Ørsnes 1988) and an existing sample from Illerup (known as CJN; see Ilkjær et al. 1994). A cross-section sample was obtained from each lancehead just above the neck (i.e. above the socket), as indicated in Fig. 12.1, using a jeweler's saw with a fine steel blade and slow cutting strokes (to reduce any heating of the iron). The samples were embedded in two-component epoxy resin (EpoxiCure) and prepared as standard metallographic blocks, ground (SiC papers 120–4000 grade), and polished (diamond lubricant) to a 0.25 μm finish. The samples were then carbon-coated for chemical analysis by SEM-EDS.

An ISIS ABT-55 scanning electron microscope equipped with an Oxford Link Analytical AN 10/55S energy dispersive spectrometer system (SEM-EDS), with a 15-kV accelerating voltage and ≈40% dead time, was used to determine the composition of entrapped slag inclusions (SI) and the metal phase. Precision and accuracy testing of the instrument was tested using the United States Geological Survey (USGS) basaltic glasses (BCR-2G, BHVO-2G, and BIR-1G). The results from accuracy and precision testing as well as more detail on the SEM-EDS setup can be found in Seetah et al. (2015). The performance of the instrument is extremely good with low quantification errors for both major oxides (around 3%) and minor oxides (around 12%). The instrument can accurately quantify down to around 0.2 wt%, with errors increasing to around 20% for element oxide concentrations at around 0.1 wt%.

The metallographic study was performed after SEM-EDS analyses, removing the carbon coating and etching the samples with nital (1% solution) as per well-established guidelines (cf. Petzo 1978). The macro- and microstructure was assessed using a metallographic optical microscope in plane-polarised light. Photo micrographs supplied in this chapter are provided with a scale bar (in micrometres), mode (BW, black and white; CLR, colour), and magnification (50×, 100×, 200×). All sample preparation and analysis were conducted at the University of Aberdeen, UK. The X-radiography of a single Havor lance and a separate spear were conducted previously by Haderslev Museum with scans provided for this investigation.

Metallographic Analysis

Having concluded that the thirteen lances sampled for this study were made using iron from different production sources (discussed after this section), this section complements the chemical analysis with a detailed metallographic study. The aim of the metallographic study is to establish if the lances were constructed using the same ironworking techniques, based on their integral features relating to manufacture. The results will make it possible to ascertain whether the same technological

Table 12.1 Metallographic summary of microstructural observations of the lance cross-sections

	Construction			Iron alloys observed						
Lance	Spiral form	Piled	Weld lines	Ferrite	Phosphoric	Low-carbon steel	Mid-carbon steel	High-carbon steel	Carburised	SI group (Table 12.3)
E1211	●		●	●	●					1
E1326	○	○	●	●	●	●				1
E1338	○	○	○	●	●	●				1
E1790	○			●	●					1
E11845	○		●	●	○	●				1
CJN	●		●	●	●	●			●	2
E1267	○	○		●		●				2
E1291	●			●	○		●	●	●	2
E1902	●		○	●	○	●				2
E2295	○	○	●	●	○	●	●		○	2
E737				●	●	●	●	●	●	3
E1986	○			●		●	●	●	○	3
E1273	●						●	●	●	4

Unfilled circles represent uncertainty

practices, or smithing tradition, were employed to manufacture the objects. This section provides a detailed synopsis of the macro- and microstructural features of the lances, namely, their construction method, iron type(s), carburisation, and heat treatment(s), a summary of which is provided in Table 12.1. Before looking at these features in detail, a note is made about their state of preservation and unfortunate effects brought about by conservation efforts.

Conservation Effects

Much of the ironwork from Ejsbøl has been conserved using Rosenberg's method, which stabilises the iron and prevents further corrosion. The technique was commonly applied to iron artefacts in Denmark until the 1990s, when it was replaced by electrolytic methods. Rosenberg's method involves first annealing the iron in a furnace at 800 °C for 30–60 min, subsequently boiling it in a solution of $NaCO_3$ and then soaking it in water for up to 2 weeks, after which the artefact is finally dried and stabilised using microcrystalline wax (cf. Buchwald 2005, 203). This method and derivatives thereof can 'clean' the metallographic record of earlier events, as the annealing process may alter original microstructures that bear valuable information concerning the cold-working, hardening, and structural features of an object (Buchwald 2005, 203).

The Havor lances from Ejsbøl were subject to the Rosenberg conservation process, which is supposed to have obliterated their original microstructures. Prolonged annealing at high temperatures, as per Rosenberg's method, should homogenise the

microstructure. This level of alteration, however, was not observed in the Ejsbøl lances. Instead, it appears that many of the lances bear remnant microstructures and features from their original state, indicating that any conservation efforts have not altered the original microstructure entirely. The heterogeneity observed in the macro- and microstructural features of the Ejsbøl lances studied must relate to the original metallographic record. This is supported by the consideration that other scholars have successfully gleaned useful information from artefacts altered by Rosenberg's conservation method (Buchwald 2005, 181, 191, 306).

The Illerup lance (CJN) studied here represents the single specimen in the sample to have maintained its microstructural integrity as it was not subjected to the Rosenberg conservation method. It therefore provides a useful comparison for the Ejsbøl lances affected by Rosenberg's method. Two main effects were identified in the Ejsbøl lances resulting from conservation annealing. Firstly, recrystallisation has transformed some of the ferrite into uniform equiaxed grains; secondly, carbon structures have become spheroidised. Some caution is needed when examining recrystallised regions, as some may be related to original annealing events (as highlighted by CJN). The fully annealed microstructure resulting from conservation observed in the Ejsbøl lances is extremely useful when juxtaposed with other observed microstructures. This is because any other observed microstructures, not consistent with full annealing, have survived the conservation process, preserving the original metallographic record and thus exposing the original metalworking that took place.

Construction

The earlier study of the Illerup lance (CJN) by Joutijärvi concluded that the metal was first flattened, bent around, and then welded together, leaving an unclosed internal cavity (Ilkjær et al. 1994, 39). The same process can be observed in the majority of Ejsbøl lances studied here, which can be best described as the 'spiral-forming' technique, owing to its spiral appearance in cross-section. 'Piled' iron refers to the process of 'piling' iron together, which is the more conservative interpretation proposed here where a spiral form is indistinct or not defined.

The spiral-forming technique is illustrated in Fig. 12.2. The iron is first worked out and flattened, then it is bent round into a cylindrical shape with the two opposing edges brought together and forge-welded. What remains unclear is whether the technique was performed for the construction of the socket only, or employed along the whole length of the lancehead. How much of the lancehead was produced from flattened sheet?

Of the thirteen lances examined, five show clear evidence of a spiral construction whilst a further seven provide a strong indication for the same process. The illustrated cross-sections of the samples examined can be seen in Fig. 12.3. The sample cross-sections, all obtained from just above the neck of the lance (minimum socket thickness) with the exception of fragment E11845 (more likely located in the blade

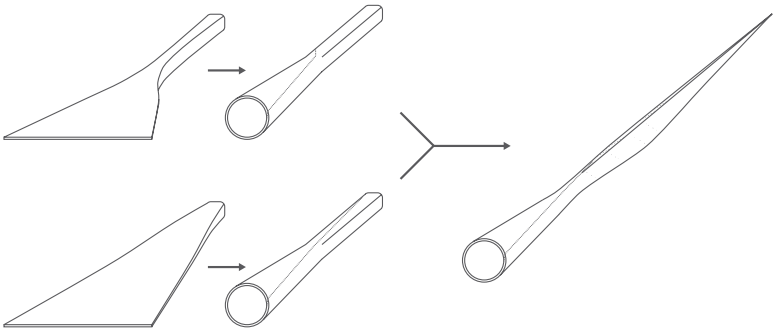

Fig. 12.2 Proposed spiral-forming construction method for the Havor lance, rolling a flattened iron sheet, which may have been used for the socket only (upper) or the whole lancehead (lower)

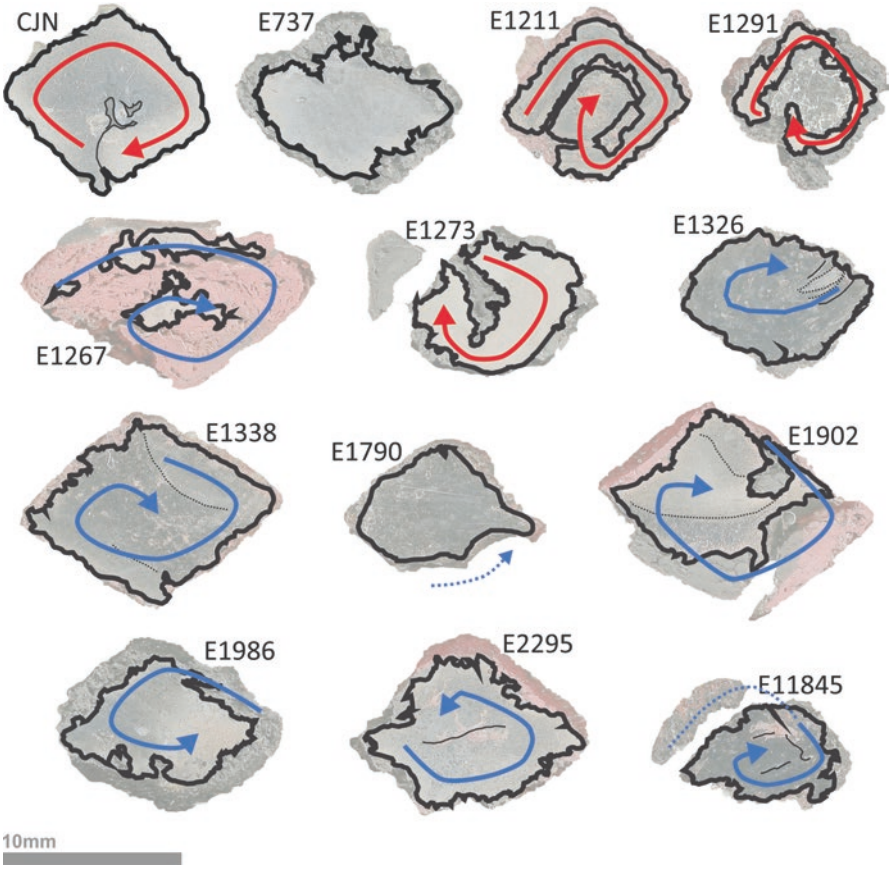

Fig. 12.3 Illustrated lance cross-sections highlighting the spiral-form construction clearly visible in some samples (red) and implied in others (blue). Uncorroded metal is outlined in black

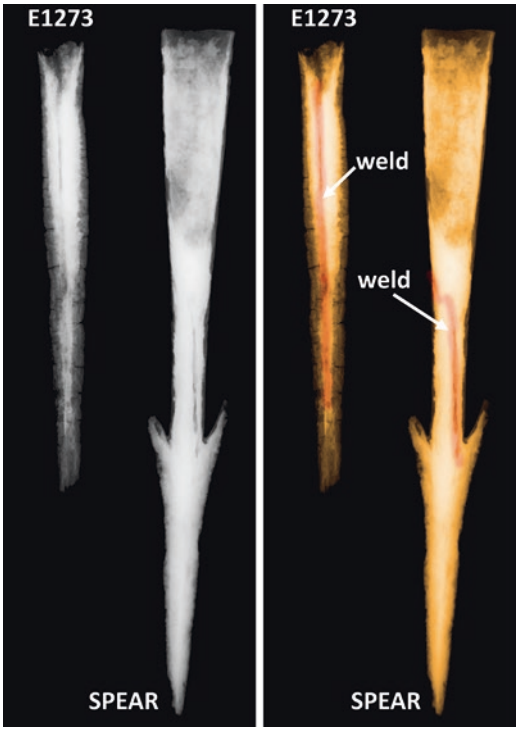

Fig. 12.4 Original (left) and artificially coloured (right) X-radiographs of Havor lance E1273 and a barbed spearhead, highlighting the weld seams visible (shown in red in the right-hand adjusted X-radiograph)

midriff), indicate that the flattened sheet forms not only the socket but also part of the lower lancehead (at least). The limitation of single samples, however, lies in extrapolating the results to an entire object. Further evidence is needed to evaluate whether the iron sheet was used to form just the socket region or the entire lancehead.

X-radiographs were available for the study of two specimens, the first of Havor lance E1273 (in this study) and the second of a long-tanged barbed spearhead, both from Ejsbøl. The original X-radiographs are shown in Fig. 12.4, complemented by identical false-coloured images highlighting the weld seams discussed. In the barbed spear, the X-radiograph reveals that only the socket was produced from flattened sheet, reaching very slightly into the head, where the weld line terminates. The Havor lance (E1273), however, shows a weld line that extends beyond the socket region and far into the lance point, indicating that most (if not all) of the head was produced from a flattened sheet.

Four of the lance cross-sections (E737, E1326, E1338, and E1790) show solid metallic bodies macroscopically (Fig. 12.3). Whilst it could be assumed that these samples were located at the threshold between the spiral-formed socket and the solid head, closer inspection reveals this not to be the case in at least two of the ‘solid’ samples. The heterogeneity observed in the macrostructure and microstructure of E1326 and E1338 provide convincing evidence that these samples were also

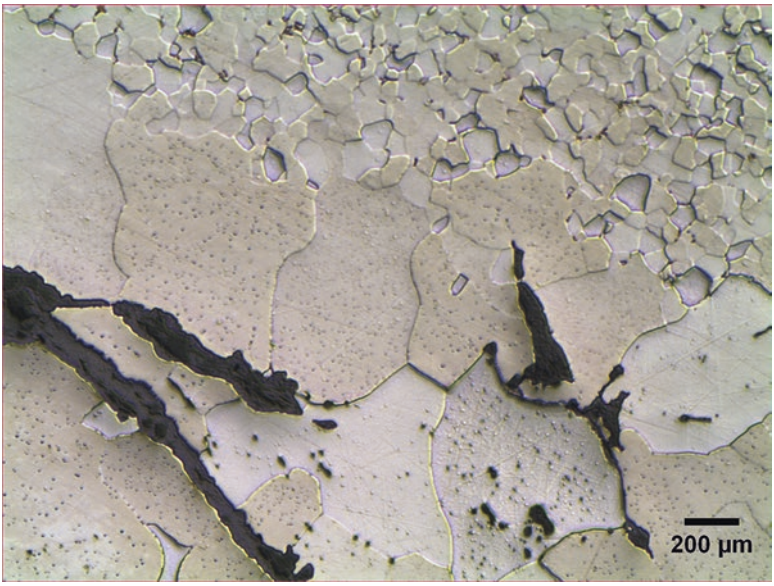

Fig. 12.5 Photo micrograph of a weld line in lance CJN, showing large ferrite grains along the weld seam neighbouring the recrystallised ferrite body (CLR 50×)

spiral-formed, showing a strong similarity to CJN except for the lack of an internal cavity. Although corrosion and cavities may provide indirect evidence for weld line interfaces (CJN, E1211, E1291, E1273, E1902, E1986, E11845), clear weld lines can be observed in the microstructure of seven lances (Table 12.1). Examples of weld lines can be seen in Figs. 12.5 and 12.6 and a piled structure in Fig. 12.7. The weld lines often show curvature, respecting the lance surface and/or spiral form, thus further supporting the proposed construction method (E1326, E1338, E1902, E2295, E11845).

The observations made for the lance cross-sections and X-radiographs show that a spiral-form construction method was used to manufacture the Havor lancehead. The rolled flattened sheet formed at least the socket, if not the point itself, as discussed above (especially in the case of E1273).

Ferritic Iron, Phosphoric Iron, and Steel

Five types of iron were identified in the samples studied: pure ferritic iron, phosphoric iron, low- (0.05–0.3% C), mid- (0.3–0.6% C), and high-carbon (0.6–1.0% C) steel. The iron types/alloys observed in each sample are labelled in Table 12.1. Pure ferritic iron is the main component for nine lances (see Fig. 12.8 for an example of recrystallised ferrite in CJN), whilst the remaining four are made from either low-carbon steel (E737) or mid- to high-carbon steel (E1273, E1291, and E1986).

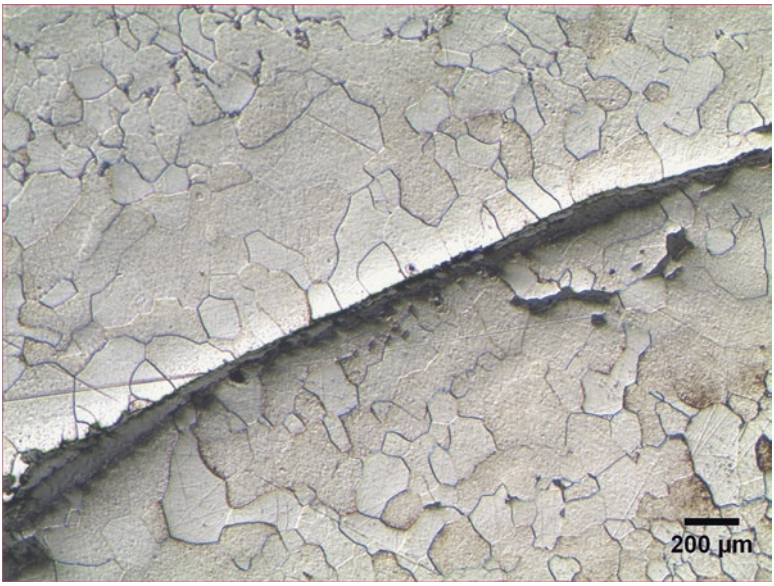

Fig. 12.6 Photo micrograph of a weld line in lance E2295, showing mostly recrystallised ferrite and some agglomerate grains along the seam (CLR 50×)

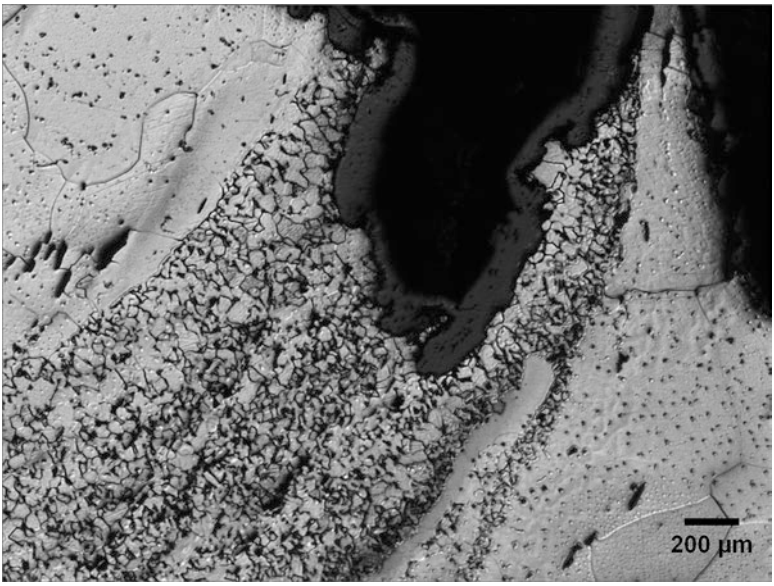

Fig. 12.7 Photo micrograph of three lamellae in a piled structure in lance E1326; the central band is fine grained, situated between larger phosphoric iron grains (BW 50×)

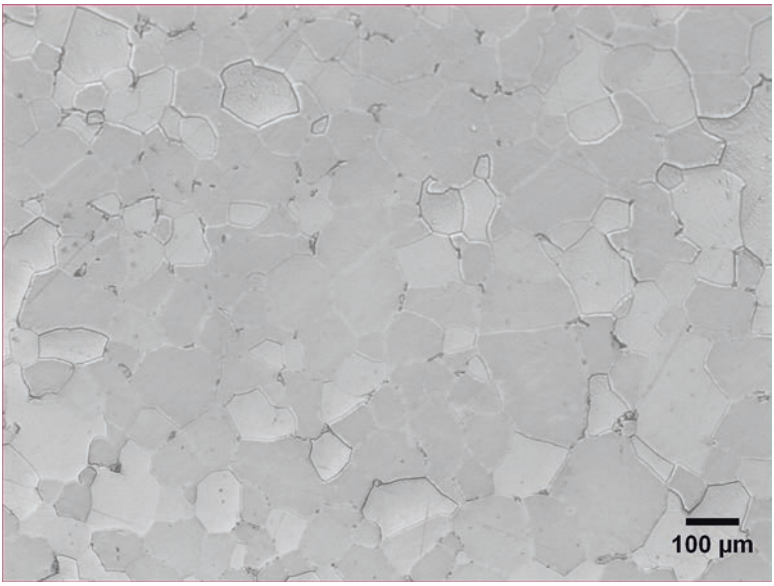

Fig. 12.8 Photo micrograph showing the predominating microstructure of recrystallised ferrite in lance CJN (CLR 100×)

A clear distinction can be made between lances containing phosphoric iron and those made from mid- to high-carbon steel. Those made from high-carbon steel (E1273, E1291, and E1986) contain no phosphorus, and inversely those made from phosphoric iron contain little or no carbon. A possible explanation for this is that phosphorus can inhibit carbon uptake or diffusion, preventing the formation of steel.

At least six of the lances contain appreciable amounts of phosphorus as shown by chemical analysis of the iron (Table 12.2). The presence of phosphoric iron was also confirmed in the microstructures of other lances, visible as 'ghosting' (Sahoo and Balasubramaniam 2007). After etching, ghost structures are visible in iron-containing phosphorus, appearing as bright or dark ghosts that do not respect the grain boundaries. The darker ghosts are phosphorus-poor, whilst the bright ghosts are phosphorus-rich. Examples of phosphoric iron microstructures can be seen in Figs. 12.9, 12.10, and 12.11.

Upon combining the evidence for phosphoric iron from chemical analysis and 'ghost structures' visible in the microstructure, it can be proposed that a possible ten of the total thirteen lances were produced using phosphoric iron. The prevalence of phosphoric iron would suggest that it was selected for the manufacture of most Havor lances due to its beneficial properties. Not only is iron hardened by phosphorus, but phosphoric iron is generally free of inclusions and flaws, produces easy welds, and is soft to work with, making it an ideal blacksmithing material in antiquity (Buchwald 2005, 173–178).

Table 12.2 Normalised SEM-EDS results of the metal composition of the lances, shown in element wt% (blank spaces, i.e. for P, are beneath detection limits)

	Metal (wt%)		
Lance	Fe	P	SI group (Table 12.3)
E1211	99.2	0.8	1
E1326	99.4	0.6	1
E1338	99.6	0.4	1
E1790	99.3	0.7	1
E11845	99.9		1
E1267	100.0		2
E1291	99.9		2
E1902	99.9		2
E2295	100.0		2
E737	99.9	0.1	3
E1986	100.0		3
E1273	99.9		4

Five points analysed per lance (E1267 $n = 13$); CJN not analysed

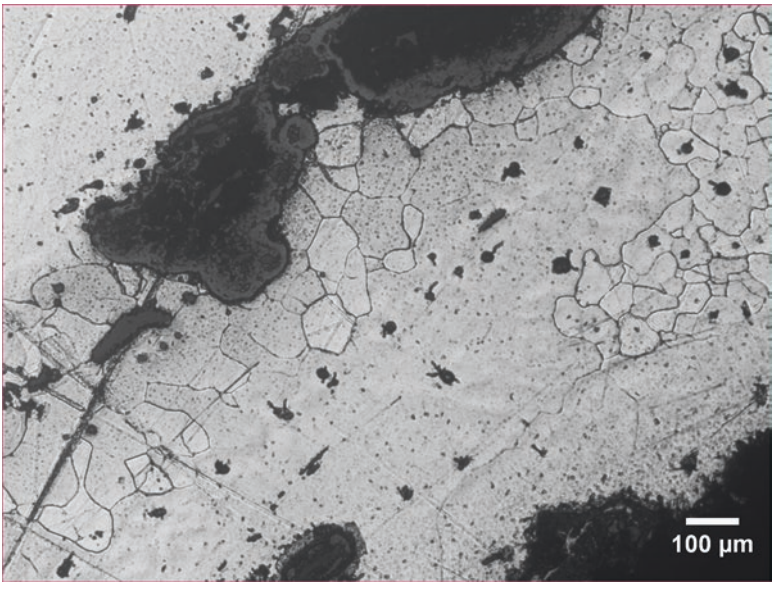

Fig. 12.9 Photo micrograph showing ghost structures (agglomerate grains) of phosphorus in ferrite in lance E1211 (BW 50×)

Many of the lances examined contain low-carbon steel parts or surfaces, which appear to be secondary and imbued during the forging process (rather than being primary to the metal stock). Only three of the lances are made from steel proper (E1273, E1291, and E1986), containing no phosphorus. The fact that three of the Havor lances were made using steel and not phosphoric iron begs the question as to

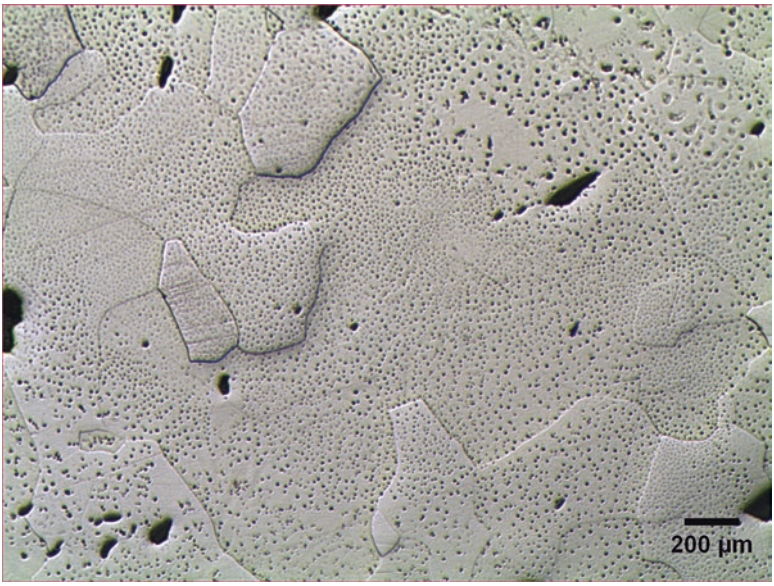

Fig. 12.10 Photo micrograph of phosphoric iron (large agglomerate grains) showing etch pitting in lance E1326 (CLR 50×)

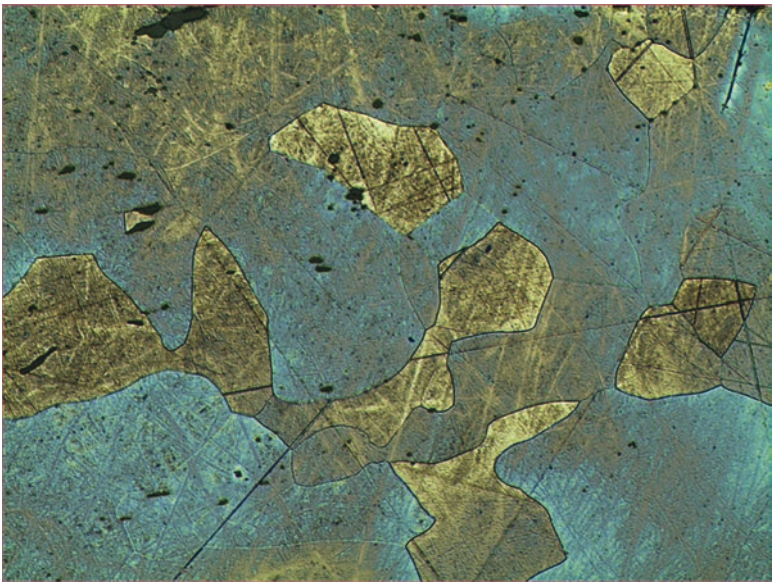

Fig. 12.11 Photo micrograph of lance E1790 showing variable reaction to the etchant, highlighting phosphoric regions in blue (CLR 50×)

Table 12.3 Weighted average composition of lance SI per area analysed (SEM-EDS results) shown in oxide wt% (CJN average calculated from results published by Arne Joutijärvi (in Ilkjær et al. 1994, 39)

			Element oxide (wt%)											
Lance	Area (μm²)	Group	Na_2O	MgO	Al_2O_3	SiO_2	P_2O_5	SO_3	K_2O	CaO	TiO_2	MnO	FeO	BaO
E1211	55,131	1	0.3	0.2	1.7	17.0	16.5	0.3	0.6	1.8	0.1	0.8	60.5	1.0
E1326	56,442	1	bd	0.1	2.6	20.1	3.3	bd	0.2	0.5	bd	0.1	72.9	bd
E1338	254,695	1	0.5	0.3	3.2	21.8	6.3	0.2	0.6	1.0	0.1	3.5	62.1	0.4
E1790	167,205	1	0.2	0.3	2.2	20.6	9.5	0.1	0.8	2.3	0.2	0.7	63.2	0.1
E11845	6857	1	0.9	0.3	4.7	18.6	4.0	0.2	1.3	1.0	0.1	0.9	67.9	0.1
CJN	–	2	0.9	0.8	5.9	26.0	0.4	–	1.1	2.7	0.2	0.3	61.8	–
E1267	11,242	2	1.0	1.3	6.3	18.9	0.5	0.1	0.5	2.3	0.2	0.2	68.8	bd
E1291	1825	2	0.7	0.3	5.6	53.0	0.5	0.3	3.1	1.8	0.2	1.3	32.9	0.3
E1902	4263	2	1.0	1.5	8.6	33.4	1.8	0.3	2.5	2.6	0.5	2.0	45.5	0.3
E2295	9478	2	0.9	1.6	6.7	25.8	0.2	0.1	1.0	1.8	0.2	0.7	60.9	0.1
E737	31,081	3	0.2	0.3	3.0	26.5	2.3	0.1	0.7	1.8	0.1	15.4	48.8	0.9
E1986	34,144	3	0.8	1.9	8.0	32.7	0.6	0.1	2.9	5.9	0.4	17.9	28.5	0.2
E1273	4293	4	2.7	4.8	15.1	58.6	0.1	bd	3.9	11.3	0.7	0.6	2.0	0.2

Dash '–' represents not analysed and 'bd' below detection limits. Group 1, high phosphorus; Group 2, low phosphorus; Group 3, high MnO and BaO; Group 4, high Al_2O_3 and CaO

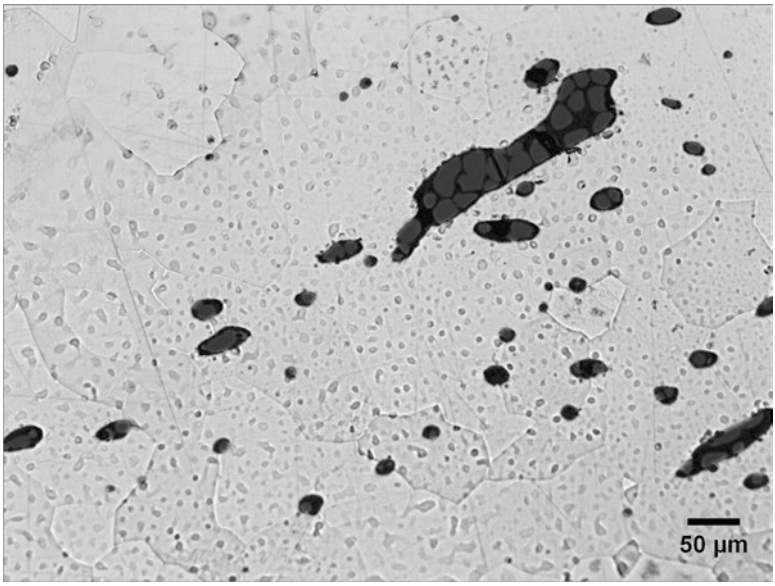

Fig. 12.12 Photo micrograph of lance E11845 showing spheroidised carbides in the microstructure (BW 200×)

why they were not all made from same type of iron. One could speculate that phosphoric iron (used for the majority of the lances) was the smith's metal of choice, and steel was a secondary alternative as it could also achieve the desired hardness.

Carburisation

The identification, location, and distribution of iron-carbon microstructures can be extremely informative, as they provide valuable insights into ancient smithing practices and hardening treatments. Some caution is urged here, however, due to the effects of conservation, which often spheroidises carbides, as is the case with Rosenberg's conservation method (see Fig. 12.12 for an example), although it does not necessarily homogenise their distribution. When iron is heated just below 723 °C for prolonged periods, the cementite (iron-carbon structures) in the iron begins to coalesce and become more rounded (spheroidised) cementite (Scott 1990, 12). It is also important to distinguish between primary carburisation, which is original carburisation from the raw iron bloom, and secondary carburisation, occurring when carbon is introduced into the iron during smithing processes. The Illerup lance (CJN) has a soft iron core with a low-carbon steel surface, providing clear evidence that this lance underwent secondary carburisation in a process known as 'case hardening', in which the iron is carburised and thus hardened from the outer surface (hence 'case') inwards.

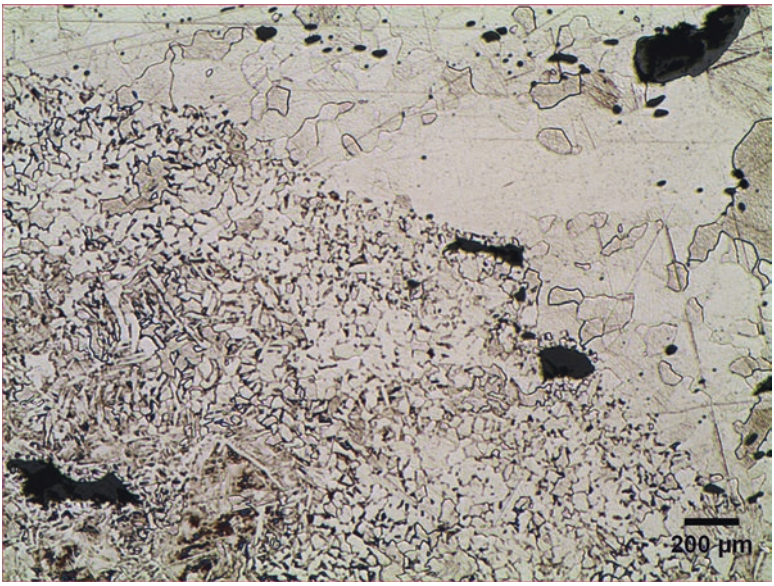

Fig. 12.13 Photo micrograph of lance E737 showing evidence of case hardening, with a fine-grained ferrite and interstitial pearlite surface casing (some visible Widmanstätten structures) surrounding a ferritic core (CLR 50×)

Of the five Ejsbøl lances showing evidence of case hardening, three are similar in character to CJN (Table 12.1). An example of case hardening can be seen in Fig. 12.13. Lance E737 is made from a low-carbon steel core with an inconsistent high-carbon steel encasing, indicating that this lance too was case-hardened. Similarly, lance E1291 has a soft iron core with a mid- to high-carbon steel encasing, showing that it was also carburised at the surface. It is not entirely clear whether carburisation was secondary in E2295, made from ferritic iron with low- to mid-carbon steel parts, as they are not confined to the surface and may thus reflect a heterogeneous distribution from the original stock (primary carburisation), or possible Rosenberg effects.

Less certain is the case of two further lances that also show signs of carburisation. Lance E1902 contains bands of low-carbon steel (fine grained ferrite with interstitial pearlite), while large carbides are prevalent in E11845 at the lance surface.

Finally, two lances are made from steel proper, which is observed throughout the microstructure (no ferritic core). Examples of low-carbon steel structures are shown in Fig. 12.14 and mid-carbon steel in Fig. 12.15. Lance E1273 is made from high-carbon steel and E1986 from mid- to high-carbon steel. This could have been achieved by prolonged carburisation in the reducing part of the hearth, allowing deep penetration, though it is more likely that the metal stock used was steel to begin with (see below).

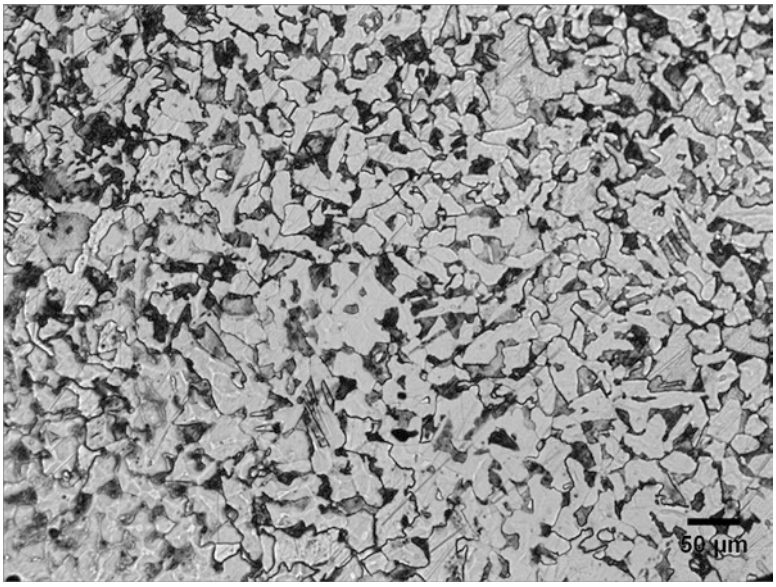

Fig. 12.14 Photo micrograph of low-carbon steel in lance E1902, showing fine-grained ferrite with interstitial pearlite (BW 200×)

Fig. 12.15 Photo micrograph of mid-carbon steel in lance E1291, showing fine-grained ferrite and pearlite (CLR 200×)

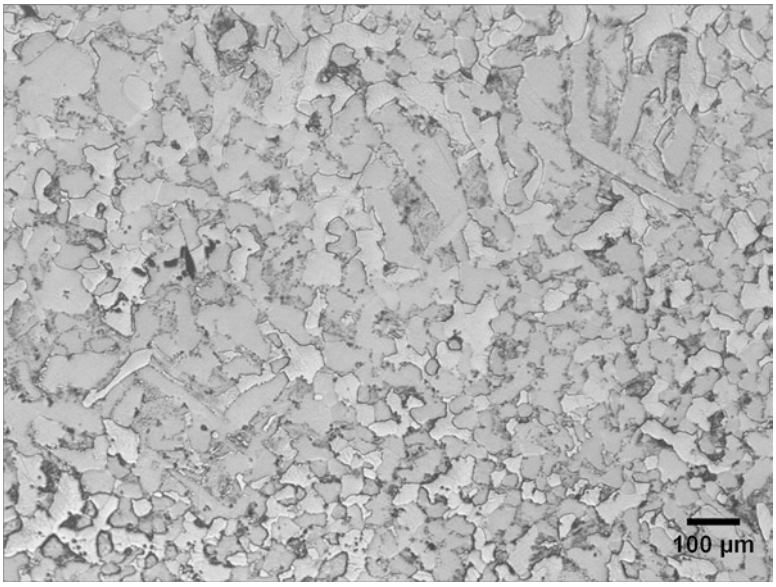

Fig. 12.16 Photo micrograph of remnant Widmanstätten structures in lance CJN, mostly lost due to later annealing (BW 100×)

Heat Treatment

Most of the ferrite observed in the Ejsbøl lances has recrystallised, and the carbon has spheroidised into carbides, both as a result of conservation annealing. Unfortunately, this appears to have removed previous traces of any heat treatment except for some remnant microstructures in the Ejsbøl lances, which are worth discussing.

This short section is devoted mainly to lance CJN, whose microstructure remains unaffected by conservation efforts. The proposed heat treatment steps associated with the ironworking for lance CJN, as interpreted by the microstructure, can be listed in order as:

1. The lance was heated long enough at or above the austenite range to allow for the growth of large ferrite grains, visible in the core of CJN's cross-section. This is probably associated with the main forge welding step of constructing the lance-head (forming the spiral), where high temperatures (around or above 900 °C) are attained during the welding process.
2. The lance was carburised through case hardening. This explains the carbon gradient from the outer surface (carburised) of CJN to the ferritic iron core (carbon-free). The lance would have been placed in the reducing part of the hearth (submerged in charcoal), forcing carbon uptake at the exposed outer surface. The depth of penetration is no more than 4 mm at its maximum, forming a mid-carbon steel surface of around 0.4% carbon. The temperature was sufficiently

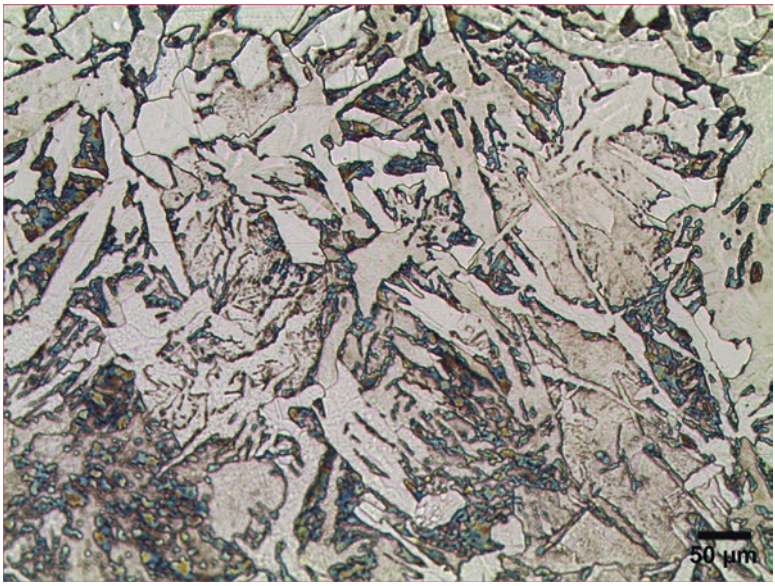

Fig. 12.17 Photo micrograph of Widmanstätten structures in lance E1986 resulting from air-cooling (CLR 200×)

high to produce Widmanstätten ferrite. Widmanstätten ferrite forms in iron-carbon alloys that have been heated in the austenite range (around 900 °C) long enough to allow for the growth of austenite grains, or by heating in the austenite range followed by air-cooling (Scott 1990, 12–14). Examples of Widmanstätten structures are shown in Figs. 12.16 and 12.17. Most of the Widmanstätten ferrite observed has been masked by the following step, leaving only elongated grains remnant of pro-eutectoid Widmanstätten ferrite.

3. The lance was then heated again, producing fine-grained ferrite at the surface, which surrounds the core of larger ferrite grains mentioned previously. This second heating appears to have been conducted at just below the spheroidising temperature (723 °C) as the interstitial pearlite visible in the low- to mid-carbon steel casing appears slightly spheroidised. This temperature would have made the iron appear 'dark cherry red'. This second heating allowed for grain refinement, transforming large ferrite grains and Widmanstätten ferrite into the equiaxed fine-grained ferrite and pearlite visible in CJN. This process of grain refinement is known as 'normalising' (Scott 1990, 12) and leads to a more homogeneous fine-grained structure. Whilst the normalising procedure has promoted grain refinement at the surface of the lance, it did not completely overwrite the former Widmanstätten structures, whose remnant forms can still be observed. The fact that the Widmanstätten ferrite was not entirely removed has helped to interpret the sequential order of heat treatments described here.

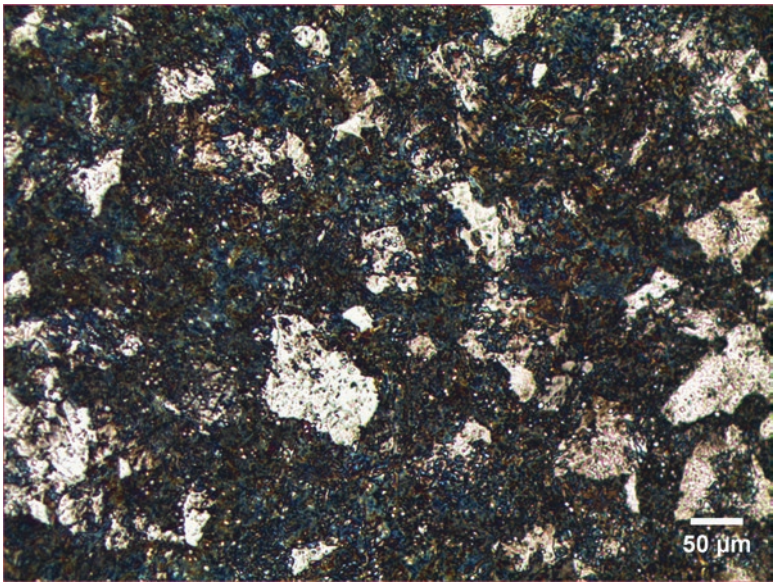

Fig. 12.18 Photo micrograph of coarse pearlite in lance E1273, indicative of slow furnace cooling (CLR 200×)

4. Finally, the lance was allowed to air-cool. The microstructures observed are consistent with air-cooling and no other microstructures indicative of quenching (i.e. martensite) can be observed.

Remnant structures visible in three of the Ejsbøl lances show similar features to CJN. Eutectoid structures with coarse pearlite can be seen in E1273, E1291, and E1986. The coarse pearlite has irresolvable lamellae of ferrite and cementite, which only form after prolonged slow cooling, often observed in furnace-cooled iron. These structures can be seen towards the centre of the lance sections, particularly in the case of E1291 (in the centre). Coarse pearlite structures are shown in Figs. 12.18 and 12.19. Annealing by the Rosenberg conservation method for 30–60 min is too short for such a microstructure to form, making these carbon-iron structures primary to the original microstructure of the lance. Coarse pearlite is commonly associated with bloomery iron, indicating that the high-carbon steel is primary to the original metal stock. This inference is important, for it means that these three lances (E1273, E1291, E1986) were not intentionally carburised as was previously suggested (whereas CJN was deliberately carburised). Lances E1273, E1291, and E1986 were made using steel that was intentionally selected to produce them.

Lance E1986 displays a variety of microstructures relating to its ancient and recent history of heat treatments. The recrystallised ferrite is largely due to the Rosenberg conservation method. Within the recrystallised regions, remnant Widmanstätten ferrite and lath martensite can be seen. Whilst Widmanstätten ferrite is indicative of air-cooling, martensite is characteristic of rapid cooling, which can

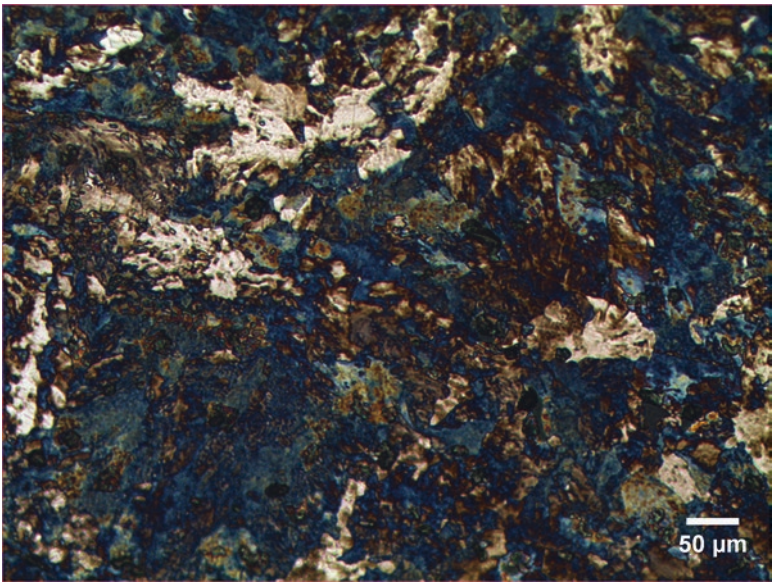

Fig. 12.19 Photo micrograph of coarse pearlite in lance E1986, indicative of slow furnace cooling (CLR 200×)

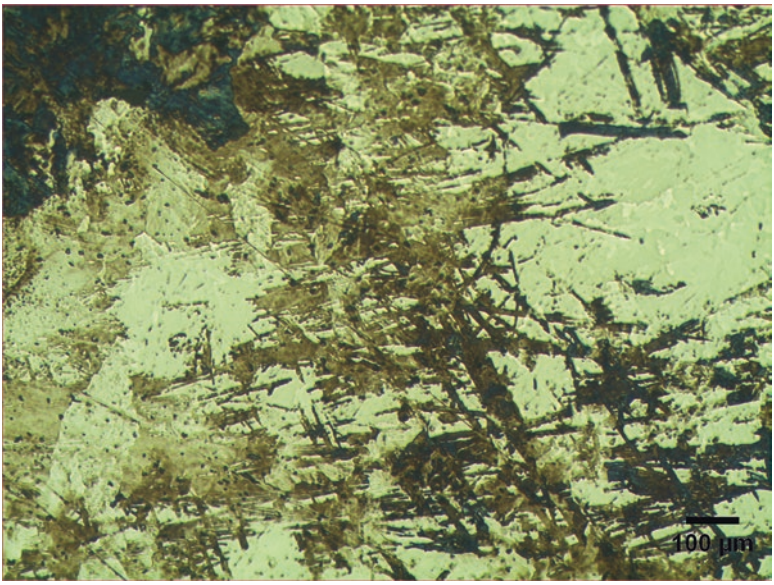

Fig. 12.20 Photo micrograph of martensite structures in lance E1986, resulting from rapid cooling, most likely quenching (CLR 100×)

only be achieved through quenching. It is unclear whether the martensite survives from the original microstructure or potentially from being quenched (in the salt bath) during Rosenberg's conservation method. Martensite is not observed in other lances >0.3% C, which would be expected if they had also been subject to the same salt bath treatment, making it more likely that the martensite observed in E1986 relates to the original ironworking. Martensite can be seen in Fig. 12.20. The lath martensite and areas of 'tempered' martensite, therefore, indicate that the iron was further heat-treated after quenching. This is consistent with Rosenberg's annealing. Using the evidence gathered thus far to formulate a reasonable working hypothesis, one could suggest that E1986 was air-cooled upon completion of forging, before being heated and quenched rapidly in some liquid (presumably water). Subsequent conservation efforts recrystallised the ferrite, though not long enough to homogenise the microstructure fully, leaving remnant microstructures such as tempered martensite.

It is difficult to arrive at a universal Havor lance heat treatment process from four Ejsbøl lances as well as CJN, and no attempt will be made here to interpret the results further. The original microstructures from CJN as well as the remnant microstructures from the Ejsbøl lances examined have provided interesting insights. Both lances CJN and E1986 were air-cooled during/after forging, while E1986 was quenched and possibly further annealed. The coarse pearlite (E1273, E1292, E1986) discussed above does not relate to any final heat treatments and only confirms these three lances to have been produced from selected steel.

Slag Inclusion Analysis

During the Late Roman/Early Germanic Iron Age, iron was produced by the 'direct' method, also known as bloomery iron smelting. This solid-state reduction process creates a by-product, slag, which is normally found in great quantities at iron production sites. Slag inclusions (SI), however, often remain entrapped in the iron produced, allowing for iron objects to be related to their production sites. By comparing the chemical composition of entrapped SI with smelting slag from iron production sites, it is possible to build provenance hypotheses, exclude possible sources, or even directly confirm an iron production source.

New and improved analytical and statistical methods have been developed over the last decade for iron provenancing by the SI method (Birch et al. 2014; Birch and Martinón-Torres 2013; Blakelock et al. 2009; Charlton et al. 2012; Charlton 2015; Coustures et al. 2003; Desaulty et al. 2009a, b; Dillman and L'Héritier 2007; Leroy et al. 2012). Whilst it is not always possible to link an iron object to a specific production source, the SI method has proved extremely useful for comparing objects with one another as well as identifying compositional groups (i.e. iron objects from the same smelting system).

One of the main issues with iron provenancing is deciding which potential sources one has to reference for comparison with the iron objects and their entrapped

SI. For the Roman Iron Age in Denmark, it has been suggested that iron, by the large part, was consumed locally near to where it was being extracted (Lyngstrøm 2008, 231). However, the distance to which iron travelled should not be underestimated. Long-distance iron bar trade is well-attested archaeologically during the Iron Age (Buchwald 2005, 102–105). One example of particular relevance from the Roman Iron Age is the site of Snorup (Jutland), where locally produced phosphoric iron bars were found along with over 200 steel bars that likely originated from the Oppland region of southern Norway (Høst-Madsen and Buchwald 1999, 64).

The context of the weapons under investigation indicates that the immediate and neighbouring regions should be investigated as potential sources of iron. This mode of investigation has previously been conducted on other iron artefacts from Iron Age Denmark, for which provenance hypotheses have been formulated using SI analysis compared to Danish iron production sites as well as other iron production areas in Scandinavia (Buchwald and Wivel 1998; Høst-Madsen and Buchwald 1999). This work has recently been reviewed and retested using multivariate statistical approaches, which demonstrate the real potential for provenancing iron more broadly by re-analysing published chemical data of iron production slags and SI using new statistical techniques (Charlton et al. 2012). Fortunately, the composition of iron production slags from Jutland are well characterised and can be distinguished from other production areas in Scandinavia.

It is important to consider, however, that iron bars may have been "traded over long distances before they reached their final destination" (Buchwald 2005, 102), which is why it is necessary to be open-minded about potential sources of iron in the widest possible terms. Therefore, the wider Northwest European region should also be considered when making provenance hypotheses, including Britain (Paynter 2006, Table 1), Germany (Ganzelewski 2000, Table 4; Heimann et al. 2001, Tables 3, 4; Spazier 2003, Table 7.1), the Netherlands (Joosten 2004, Tables 14–16), and the wider Baltic area including Poland (Buchwald 2005) and Lithuania (Navasaitis et al. 2003, Tables 16.3, 16.4; Navasaitis and Selskienė 2007, Table 4).

The analysis conducted here first proceeds by investigating possible lance groups as characterised by the chemical composition of their SI. This is followed by a comparison of the SI with iron production sources from Scandinavia in order to construct provenance hypotheses for the origins of the iron used to manufacture the Havor lance.

Identifying Compositional Groups

Lance SI compositions are characterised by several noteworthy differences that distinguish four broad groups. The weighted average SI composition (cf: Dillman and L'Héritier 2007, 1816) for each lance is given in Table 12.3. Before outlining these groups, it is worth briefly describing the likely origins of the different element oxide components in the SI compositions being discussed. During iron smelting, the three oxides heavily influenced by clay furnace lining contributions are TiO_2, Al_2O_3, and

SiO_2, whilst the alkali earth compounds (K_2O, MgO, CaO) are enriched by fuel ash contributions. P_2O_5, MnO, and BaO, on the other hand, most likely originate from the iron ore being smelted.

The first and most notable quantitative difference is the range of MnO and BaO values. Lances E737 (15.4 wt%) and E1986 (17.9 wt%) have notably high MnO concentrations, followed by E1338 (3.5 wt%), whilst the remainder are generally around or below 1 wt%. Similarly, lances E737 (0.9 wt%) and E1338 (0.4 wt%) show some of the highest BaO values in the sample, with E1211 (1.0 wt%) having the highest concentration. As MnO and BaO derive largely from iron ore contributions to SI composition, these immediately apparent differences preclude a single-source production hypothesis. The results almost certainly indicate a high-Mn ore used for at least two lances (E737, E1986), which may also correspond with BaO. It is interesting that these two lances, labelled here as 'Group 3' (high MnO and BaO), correspond directly with the high-carbon steel microstructure discussed above.

Another characteristic trait worth noting is phosphorus content. Five lances (E1211, E1326, E1338, E1790, and E11845) show elevated P_2O_5 concentrations in their SI composition ranging from 3.5 wt% to around 16.5 wt%. These five lances, labelled here as 'Group 1' (high phosphorus), all correspond directly with the phosphoric iron microstructures observed in the metallographic study. With the exception of two intermediate values (E737, E1902) with around 2 wt% P_2O_5, the remainder of the lances are phosphorus-poor and contain around/less than 0.5 wt%.

The other main group consists of the five phosphorus-poor lances (CJN, E1267, E1291, E1902, E2295), labelled here as 'Group 2', which appear to be relatively consistent in their alumina (6–9 wt%) content, as well as lime (CaO) content of around 2–3 wt%. This group is generally more enriched in MgO, K_2O, and TiO_2 when compared to the phosphorus-rich (Group 1) lances. It is also worth noting that the phosphorus-poor Group 2 lances, whilst having phosphoric iron microstructures, can be distinguished from Group 1 lances by their microstructure. Group 1 lances contain low-carbon alloy microstructures only, whilst Group 2 lances show evidence for carburisation and the presence of mid- to high-carbon alloy microstructures.

Lance E1273 has a unique SI composition that sets it apart from all the other lances analysed: it is the most enriched in MgO (4.8 wt%), K_2O (3.9 wt%), and CaO (11.3 wt%) and is also characterised by a high alumina (aluminium oxide) content (15.1 wt%), most likely from furnace lining contributions.

Overall, the chemical composition of lance SI strongly suggests that these objects were produced using different stock iron originating from different smelting systems. In other words, the iron used in their making does not derive from the same iron production site.

Preliminary Provenance Hypotheses

In order to provenance the iron used for lance manufacture, Buchwald's (2005; Buchwald and Wivel 1998; Høst-Madsen and Buchwald 1999) bivariate approach is used here, which compares K_2O/MgO and SiO_2/Al_2O_3 ratios of the weighted

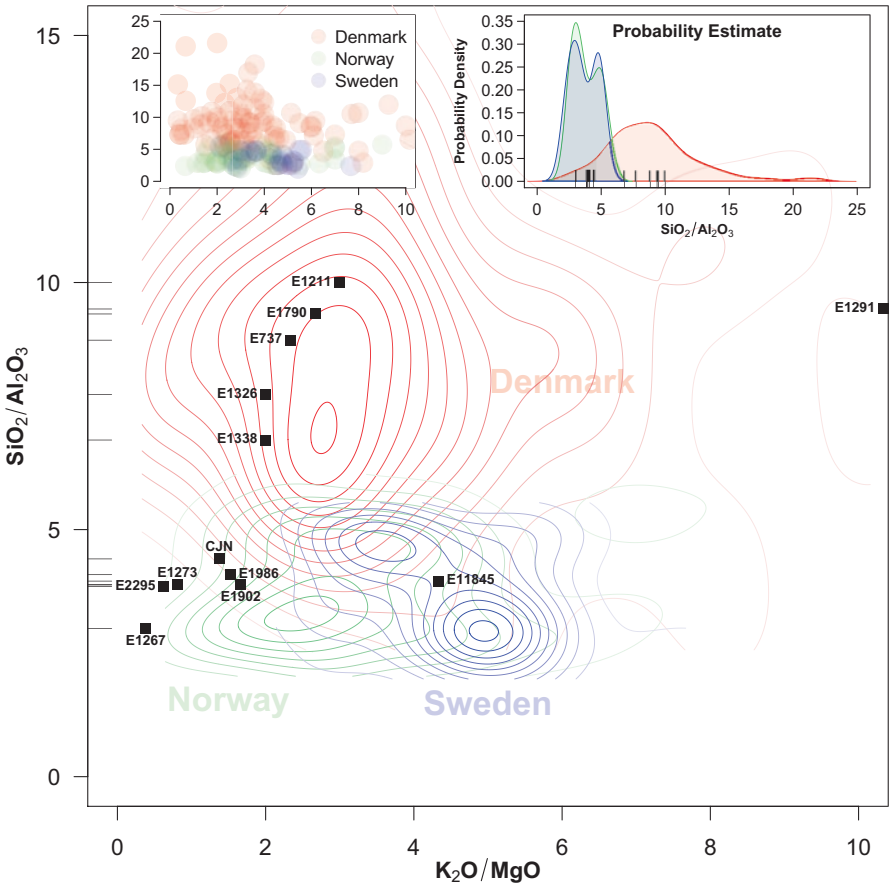

Fig. 12.21 Bivariate scatterplot of SiO_2/Al_2O_3 against K_2O/MgO with weighted average lance SI plotted as points and iron production sources represented as a contour plot (raw data points shown in the embedded plot, top left). Probability density plot of iron production regions (embedded, top right) with rug marks along the x axis (SiO_2/Al_2O_3) corresponding with lances; the same rug marks shown in the main plot along the y axis

average lance SI compositions against iron production slags, as shown in Fig. 12.21. The iron production slags used as reference data to produce Figs. 12.21 and 12.22 are published in Buchwald (2005, Tables 6.2, 6.4, 7.1, 7.6, 8.1, 8.2, 8.4, 9.1, 9.3, 9.4, 9.5, 10.1, 10.5, 10.7, 10.8, 12.8, 12.11). As Fig. 12.21 shows, iron production sites from Jutland (and wider Denmark) can be relatively well-distinguished from iron production sites in Norway and Sweden.

Eleven of the thirteen lances plot in two different areas in the bivariate scatterplot, corresponding to two different regional provenances (Fig. 12.21). Five lances (E737, E1211, E1326, E1338, E1790) plot in the Danish region along the highest probability of the SiO_2/Al_2O_3 density curve (Fig. 12.21), with four corresponding nicely with the phosphorus-rich Group 1 previously identified. Phosphoric iron,

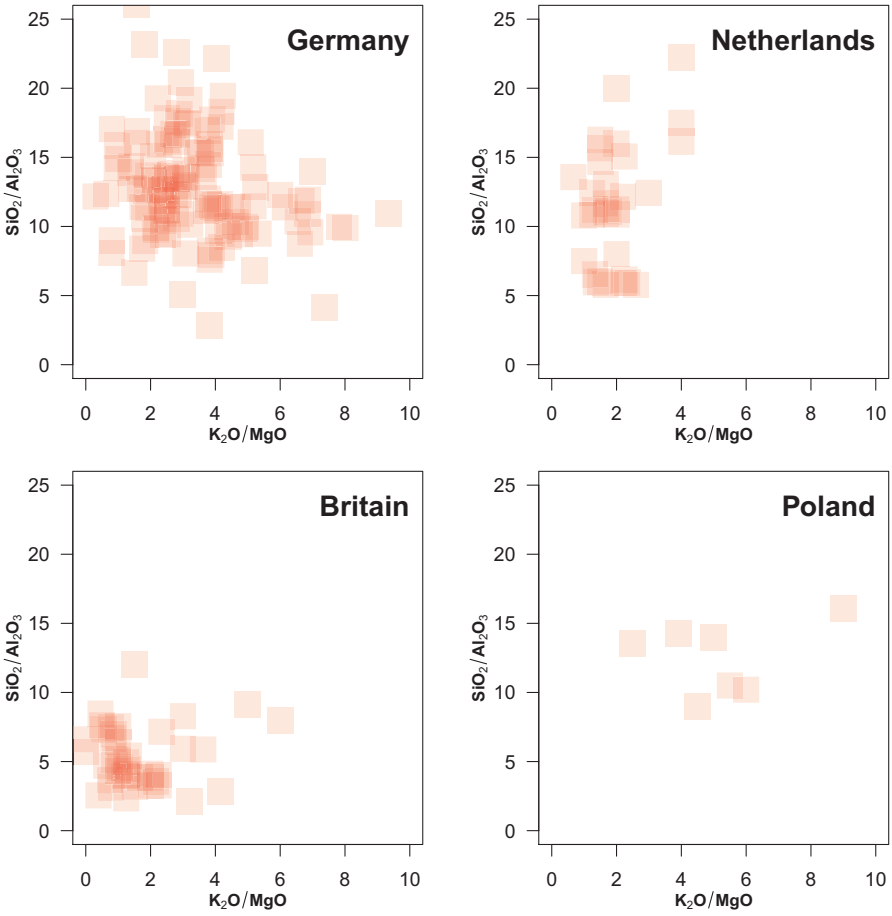

Fig. 12.22 Bivariate scatterplot of SiO_2/Al_2O_3 against K_2O/MgO for other iron production sites in Northern Europe, highlighting overlaps with Denmark, Norway, and Sweden

such as that used for this group of lances, is known to have been produced in Denmark during the Roman Iron Age (Høst-Madsen and Buchwald 1999).

Six lances (CJN, E1273, E1267, E1902, E1986, E2295) plot in the Norwegian region of the K_2O/MgO ratio. However, their position in the probability density curve for SiO_2/Al_2O_3 can be characterised as the Scandinavian Peninsula more generally due to the overlap of Norway and Sweden. These lances correspond well with the Group 2 (phosphorus-poor) and Group 3 (high MnO and BaO) lances, which represent mid- to high-carbon steel alloys. Steel, such as that used for this group of lances, was produced in southern Norway during the Roman Iron Age (Høst-Madsen and Buchwald 1999).

Lance E1291 can tentatively be ascribed to Denmark based on its close proximity to Danish iron production slags. Lance E11845 could possibly be ascribed to the

Scandinavian Peninsula based on its position in the SiO_2/Al_2O_3 probability density curve. However, its composition is more comparable to the Group 1 (phosphorus-rich) lances, and its position in the scatterplot is also in close proximity with iron production slags from Denmark.

When additional areas outside Scandinavia are incorporated into the analysis, the interpretation is further complicated due to overlapping data. The published data for Britain, Germany, the Netherlands, and Poland (previously referenced) are shown in Fig. 12.22. As is clear from this figure, the production slags from Germany, the Netherlands, and Poland are indistinct from Denmark, as Britain is from Norway, making it impossible to exclude these areas as potential sources, based on the analysis of the major and minor oxide components alone. Future work using trace element composition will help to refine subregional provenance hypotheses. The major and minor oxide components presented here are sufficient for making the initial argument that the iron used to produce these lances come from multiple sources.

Conclusion

This study has provided new insights into the organisation and practices of weapon manufacture in Iron Age southern Scandinavia. Although the study is limited to only thirteen lances (twelve from the same site), the figure represents nearly 10% of the total Havor lances known to date, and the results provide invaluable information about the material available to weapon smiths, as well as their smithing practices.

The metallographic and slag inclusion (SI) analysis has broadly identified four different groups, corresponding partly with the types of iron being used. The apparent inverse correlation between phosphoric iron and steel, highlighted by the SI analysis, is especially worth noting. Those lances made using mid-to high-carbon steel do not show any real evidence for internal weld lines or piling, indicating that they were each made from a single steel stock. The microstructure of the steel also indicates this to be directly produced from the furnace (primary carburisation). Conversely, those lances made with phosphoric or ferritic iron (or low-carbon steel) show increased evidence for weld lines and piling.

The metallographic investigation shows that the Havor lances share the same spiral-form construction method as well as other similarities in ironworking practices. This further supports the findings of a previous paper of mine, which suggests that the standardised appearance and form of the lance is matched by a standard construction technique (Birch and Martinón-Torres in press). For this paper, a traditional metric analysis of Havor lance dimensions was conducted on over 120 examples from three different archaeological sites, further complemented by a geometric morphometric (GMM) analysis of their overall two-dimensional shape and their symmetry.

If the Havor lances were to have been produced by different smiths or workshops, this should be shown by the metric, GMM, or metallographic analysis in the form of different construction methods or high degrees of variation associated with

human copy errors. Instead, the results from the metric analysis depict a highly standardised weapon (based on the coefficient of variation of different measurements), while the GMM analysis was unable to find any statistically significant difference between lances from different sites (based on their shape). These results point towards a scenario in which all Havor lances were manufactured in a single, or very few, specialised workshops. The data discussed in this chapter add depth to this picture by showing that, whilst all lances were likely manufactured in a specialised workshop, the iron used to make them came from multiple sources.

It now appears that the workshop(s) would have produced near-identical Havor lances using phosphoric iron, ferritic iron (or low-carbon steel) as well as steel proper. The provenance hypotheses discussed above suggest that multiple sources from across southern Scandinavia were used to supply iron for constructing the lances. In general, the data seem to suggest that two different iron alloys from two distinct regional sources were being used: phosphoric iron from Denmark and steel from southern Norway. The SI analysis not only supports the differences observed in the microstructure of the objects but has also helped to trace the material origins of the iron to the wider region.

Based on the combined results of the previous and present research, it appears that the Havor lance embodies a juxtaposition of technological standardisation and difference. The overall construction, form, and appearance of the lance are highly standardised, whilst the material used in its making is not. There is thus a clear dichotomy between the non-uniform material with which the Havor lance was made and its uniform appearance and manufacturing process.

One of the most interesting results of the research lies in the implications that such a standardised manufacture has for the interpretation of iron trade during this time. The uniform appearance and manufacture of the Havor lance is at odds with the chemical analysis of SI and the microstructures observed, which reveal that they were not all constructed using the same stock iron. Why they were not made from the same metal remains unclear. The different types of iron being used may attest to differential availability of, or access to, the raw materials used to make the same weapon product. One could speculate that this pattern reflects a demand for iron that could not be met by a single supplier, which would have led to the need to diversify procurement strategies as to include iron from multiple sources, some of which lay further afield from the workshop. This in turn reflects even more positively on the capability and practices of the weapon smiths, for they were able to produce the same standardised product using different raw materials with inherently different chemical compositions and mechanical properties.

Acknowledgements This chapter has been reworked from the author's doctoral thesis entitled "The Provenance and Technology of Iron Age War Booty from Southern Scandinavia" (University of Aberdeen 2013). Many thanks are due to Peter Crew, Mike Charlton, Keith Dobney, and Thilo Rehren for their input and comments on the original work. Special thanks go to Arne Joutijärvi for his immense efforts in assisting with sampling the lances and gaining access to new material for study. This work was made possible only through the permission granted by Hans Christian Andersen, on behalf of Haderslev Museum (Denmark), to sample lances from Ejsbøl. Thanks are also due to Mark Gourlay and John Still at the University of Aberdeen for their assistance in

sample preparation and SEM-EDS analysis. Finally, I would like to thank the reviewers for their comments and suggestions in improving this chapter. The final write-up of this research was supported by funding from the Danish National Research Foundation under the grant DNRF119 - Centre of Excellence for Urban Network Evolutions (UrbNet).

References

Bemmann, G., & Bemmann, J. (1998a). *Der Opferplatz von Nydam: Die Funde aus den älteren Grabungen: Nydam-I und Nydam-II. Band 1: Text*. Neumünster: Wachholtz.

Bemmann, G., & Bemmann, J. (1998b). *Der Opferplatz von Nydam: Die Funde aus den älteren Grabungen: Nydam-I und Nydam-II. Band 2: Katalog und Tafeln*. Neumünster: Wachholtz.

Birch, T., & Martinón-Torres, M. (2013). The iron bars from the "Gresham Ship": Employing multivariate statistics to further slag inclusion analysis of ferrous objects. In J. Bayley, E. Blakelock, & D. Crossley (Eds.), *Iron and ironworking: Proceedings of the archaeometallurgy conference, Bradford, November 2010*. London: Historical Metallurgy Society.

Birch, T., & Martinón-Torres, M. (in press). From traditional to geometric morphometrics: Standardisation of the Iron Age "Havor" lance from the famous weapon deposits of southern Scandinavia. *Journal of Archaeological Science.*

Birch, T., Charlton, M. F., Biggs, L., Stos-Gale, Z. A., & Martinón-Torres, M. (2014). The cargo. In J. G. Milne & D. Sully (Eds.), *The Gresham Ship Project: A 16th-Century Merchantman wrecked in the Princes Channel, Thames Estuary. Volume II: Contents and Context* (Nautical Archaeology Society Monograph Series, Vol. 5 / British Archaeological Reports, British Series, Vol. 606, pp. 53–70). Oxford: Archaeopress.

Blakelock, E., Martinón-Torres, M., Veldhuijzen, H. A., & Young, T. (2009). Slag inclusions in iron objects and the quest for provenance: An experiment and a case study. *Journal of Archaeological Science, 36*, 1745–1757.

Buchwald, V. F. (2005). *Iron and steel in ancient times*. Copenhagen: The Royal Danish Academy of Sciences and Letters.

Buchwald, V. F., & Wivel, H. (1998). Slag analysis as a method for the characterization and provenancing of ancient iron objects. *Materials Characterization, 40*, 73–96.

Charlton, M. F. (2015). The last frontier in "sourcing": The hopes, constraints and future for iron provenance research. *Journal of Archaeological Science, Scoping the Future of Archaeological Science: Papers in Honour of Richard Klein, 56*, 210–220. https://doi.org/10.1016/j.jas.2015.02.017.

Charlton, M. F., Blakelock, E., Martinón-Torres, M., & Young, T. (2012). Investigating the production provenance of iron artifacts with multivariate methods. *Journal of Archaeological Science, 39*, 2280–2293.

Coustures, M. P., Béziat, D., & Tollon, F. (2003). The use of trace element analysis of entrapped slag inclusions to establish ore-bar iron links: Examples from two Gallo-Roman iron-making sites in France (Les Martyrs, Montagne Noire, and Les Ferrys, Loiret). *Archaeometry, 45*, 599–613.

Desaulty, A.-M., Dillmann, P., L'Héritiera, M., Gratuze, B., Joron, J.-L., & Fluzin, P. (2009a). Does it come from the Pays de Bray? Examination of an origin hypothesis for the ferrous reinforcements used in French medieval churches using major and trace element analyses. *Journal of Archaeological Science, 36*, 2445–2462.

Desaulty, A.-M., Mariet, C., Dillmann, P., Joron, J.-L., Gratuze, B., Carlier, C. M.-L., & Fluzin, P. (2009b). Trace element behaviour in direct-and indirect-iron metallurgy: The case of Pays de Bray (France). In P. Craddock, A. Giumlia-Mair, & A. Hauptman (Eds.), *Selected Papers from the 2nd International Conference "Archaeometallurgy in Europe" 2007, 17–21 June 2007, Aquileia, Italy*. Milan: Associazione Italiana di Metalurgia.

Dillman, P., & L'Héritier, M. (2007). Slag inclusion analyses for studying ferrous alloys employed in French medieval buildings: Supply of materials and diffusion of smelting processes. *Journal of Archaeological Science, 34*, 1810–1823.

Ganzelewski, M. (2000). Archäometallurgische Untersuchungen zur frühen Verhüttung von Raseneisenerzen am Kammberg bei Joldelund, Kreis Nordfriesland. In A. Haffner, H. Jöns, & J. Reichstein (Eds.), *Frühe Eisengewinnung in Joldelund, Kr. Nordfriesland: Ein Beitrag zur Siedlungsund Technikgeschichte Schleswig-Holsteins. Teil 2: Naturwissenschaftliche Untersuchungen zur Metallurgie- und Vegetationsgeschichte* (Universitätsforschungen zur prähistorischen Archäologie, Vol. 59, pp. 3–100). Bonn: Habelt.

Heimann, R. B., Kreher, U., Spazier, I., & Wetzel, G. (2001). Mineralogical and chemical investigations of bloomery slags from prehistoric (8th century BC to 4th century AD) iron production sites in Upper and Lower Lusatia, Germany. *Archaeometry, 43*, 227–252.

Høst-Madsen, L., & Buchwald, V. F. (1999). The characterization and provenancing of ore, slag and iron from the Iron Age settlement at Snorup. *Historical Metallurgy, 33*, 57–67.

Ilkjær, J. (1990a). *Illerup Ådal: Die Lanzen und Speere. Textband*. Moesgård: Jysk Arkæologisk Selskab.

Ilkjær, J. (1990b). *Illerup Ådal: Die Lanzen und Speere. Tafelband*. Moesgård: Jysk Arkæologisk Selskab.

Ilkjær, J. (2000). *Illerup Ådal – Archaeology as a magic mirror*. Moesgård: Jysk Arkæologisk Selskab.

Ilkjær, J. (2003). Danish war booty sacrifices. In L. Jørgensen, B. Storgaard, & L. G. Thomsen (Eds.), *The spoils of victory: The North in the shadow of the Roman empire* (pp. 44–65). København: Nationalmuseet.

Ilkjær, J. (2008). Die Funde aus Illerup Ådal – Der Stand der Forschung im Jahr 2006. In A. Abegg-Wigg, C. Radtke, & A. Rau (Eds.), *Aktuelle Forschungen zu Kriegsbeuteopfern und Fürstengräbern im Barbaricum* (pp. 19–24). Neumünster: Wachholtz.

Ilkjær, J., Jouttijärvi, A., & Andresen, J. (1994). *Illerup Ådal: Proveniensbestemmelse af jern fra Illerup ådal – et piloprojekt*. Moesgård: Jysk Arkæologisk Selskab.

Joosten, I. (2004). *Technology of early historical iron production in the Netherlands, geoarchaeological and bioarchaeological studies 2*. Amsterdam: Vrije Universiteit.

Jørgensen, L., Storgaard, B., & Thomsen, L. G. (Eds.). (2003). *The spoils of victory: The North in the shadow of the Roman empire*. København: Nationalmuseet.

Leroy, S., Cohen, S. X., Verna, C., Gratuze, B., Téreygeol, F., Fluzin, P., Bertrand, L., & Dillmann, P. (2012). The medieval iron market in Ariège (France). Multidisciplinary analytical approach and multivariate analyses. *Journal of Archaeological Science, 39*, 1080–1093.

Lyngstrøm, H. (2008). *Dansk Jern: En kulturhistorisk analyse af fremstilling, fordeling og forbrug*. København: Det kongelige nordiske Oldskriftselskab.

Navasaitis, J., & Selskienė, A. (2007). Iron smelting techniques in the Virbaliūnai ancient settlement. *Archaeologia Baltica, 8*, 387–395.

Navasaitis, J., Sveikauskaite, A., Selskis, A., & Matulionis, E. (2003). Ironmaking techniques during the roman period in Lithuania. In L. C. Nørbach (Ed.), *Prehistoric and medieval direct iron smelting in Scandinavia and Europe: aspects of technology and science, Acta Jutlandica* (pp. 87–94). Aarhus: Aarhus University Press.

Ørsnes, M. (1988). *Ejsbøl I: Waffenopferfunde des 4.-5. Jahrh. nach Chr*. København: Det Kongelige Nordiske Oldskriftselskab.

Paynter, S. (2006). Regional variations in bloomery smelting slag of the Iron Age and Romano-British periods. *Archaeometry, 48*, 271–292. https://doi.org/10.1111/j.1475-4754.2006.00256.x.

Petzo, G. (1978). *Metallographic etching: Metallographic and ceramographic methods for revealing microstructure*. Metals Park: American Society for Metals.

Sahoo, G., & Balasubramaniam, R. (2007). On phase distribution and phase transformations in phosphoric irons studied by metallography. *Metallurgical and Materials Transactions A: Physical Metallurgy and Materials Science, 38*, 1692–1697. https://doi.org/10.1007/s11661-007-9227-1.

Scott, B. G. (1990). *Early Irish ironworking*. Ulster: Ulster Museum.

Seetah, K., Birch, T., Calaon, D., & Čaval, S. (2015). Colonial iron in context: The Trianon slave shackle from Mauritius. *Archaeological and Anthropological Sciences*, *9*(3) 419–430. https://doi.org/10.1007/s12520-015-0295-7.

Spazier, I. (2003). The Germanic iron-smelting complex at Wolkenberg in lower Lausacia, southern Brandenburg. In L. C. Nørbach (Ed.), *Prehistoric and medieval direct iron smelting in Scandinavia and Europe: Aspects of technology and science* (Acta Jutlandica, pp. 37–42). Aarhus: Aarhus University Press.